Novel Environmental Barrier Coatings for the protection of SiC components

Ben Kowalski, Jamesa Stokes

NASA Glenn Research Center
Cleveland, OH

ICACC 2020

Daytona Beach, FL

01 / 26-31 / 2020

Enabling Next-Generation Flight

- CMC’s allows for higher temperatures
  - Higher temperatures increase efficiency
  - However, still susceptible to degradation from oxidation, water vapor, FOD, Ca-Mg-Al-silicate (CMAS), etc.

Enabling Next-Generation Flight

- CMC's allows for higher temperatures
  - Higher temperatures increase efficiency
  - However, still susceptible to degradation from oxidation, water vapor, FOD, Ca-Mg-Al-silicate (CMAS), etc.
- Environmental barrier coatings (EBC)
  - Currently in ~3rd generation of EBC materials
  - Slows the rate of attack, but attack still occurs
  - Combination of failure modes exist due to external and internal interfaces
    - Chemical compatibility (adherence of scale)
    - CTE Mismatch
    - Thermally grown oxide (TGO)
    - Interaction with CMAS → Apatite
      - More stable than silicates

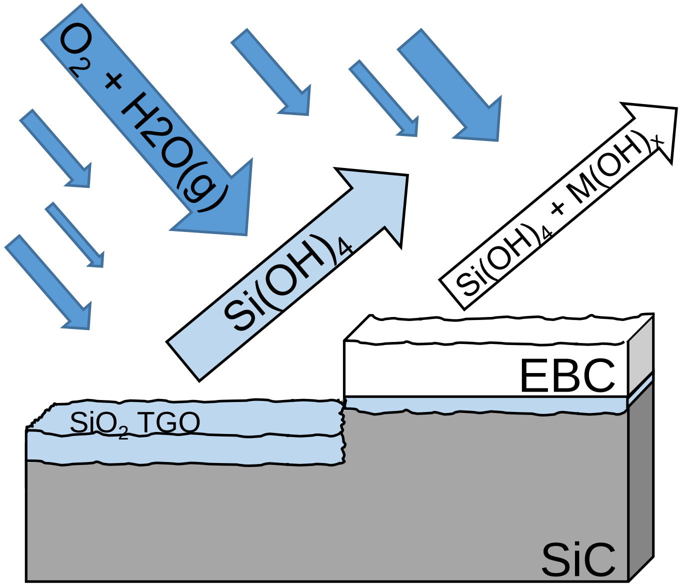

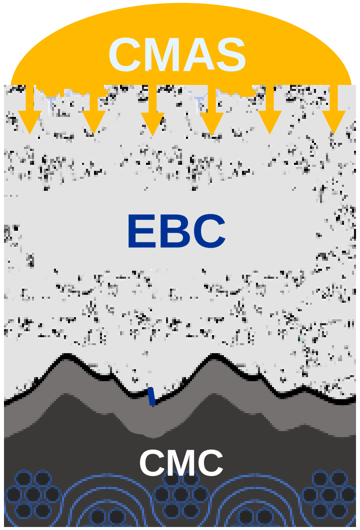

Enabling Next-Generation Flight

- CMC's allows for higher temperatures
  - Higher temperatures increase efficiency
  - However, still susceptible to degradation from oxidation, water vapor, FOD, Ca-Mg-Al-silicate (CMAS), etc.
- Environmental barrier coatings (EBC)
  - Currently in ~3rd generation of EBC materials
  - Slows the rate of attack, but attack still occurs
  - Combination of failure modes exist due to external and internal interfaces
    - Chemical compatibility (adherence of scale)
    - CTE Mismatch
    - Thermally grown oxide (TGO)
    - Interaction with CMAS → Apatite
- ***Presentation is primarily concerned with investigating water vapor induced volatilization***

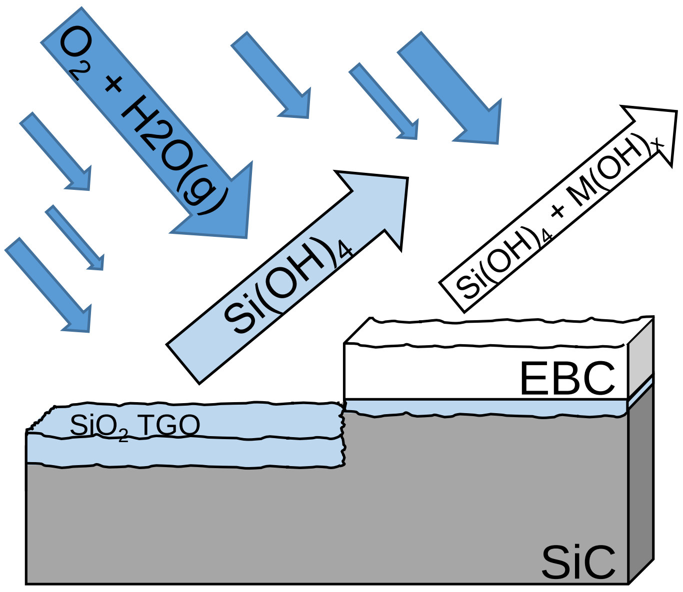

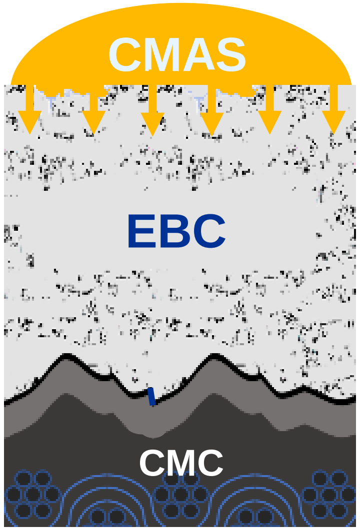

Stability of $AE_2RE_8(SiO_4)_6O_2$

- Apatite is a by-product of reaction with CMAS
  - More stable phase
- Costa (2019) → Enthalpy of formation (ΔH_f) of the apatites from the base oxides more stable with increasing c/a ratio
  - Either from an increasing AE or RE cation radius
  - Only indicates more stability than base oxides
- However, when incorporating water vapor reactions, bond energy plays a role
  - Shorter bonds → stronger bonds
- Influence of thermodynamics and kinetics on the stability of apatites in water vapor

AE = Alkaline element, RE = Rare Earth

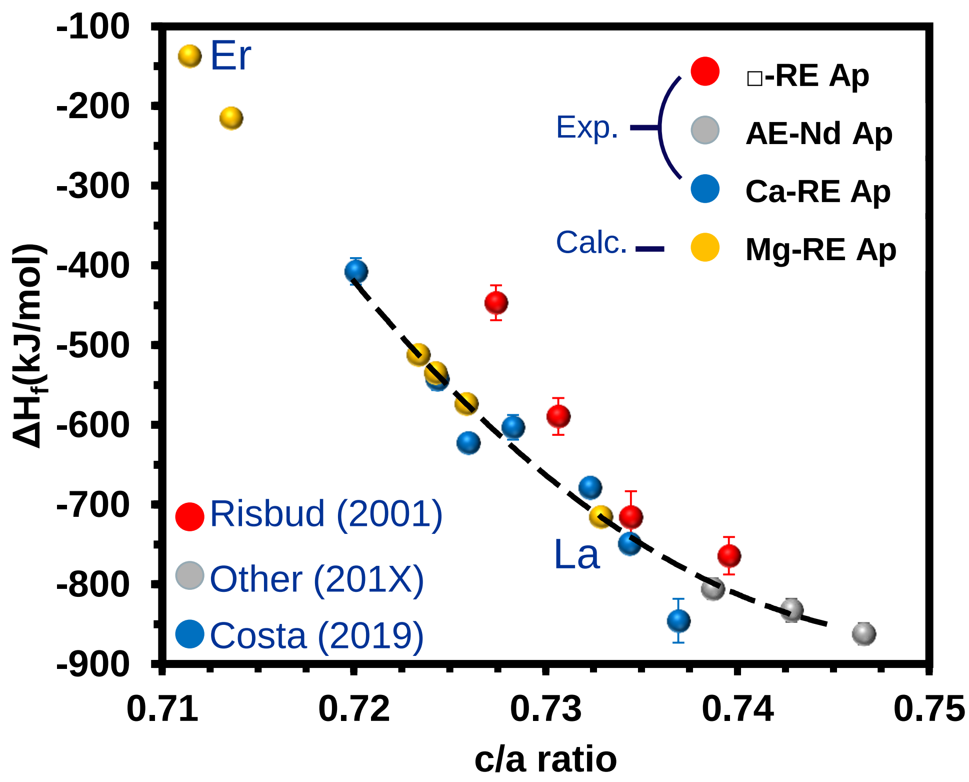

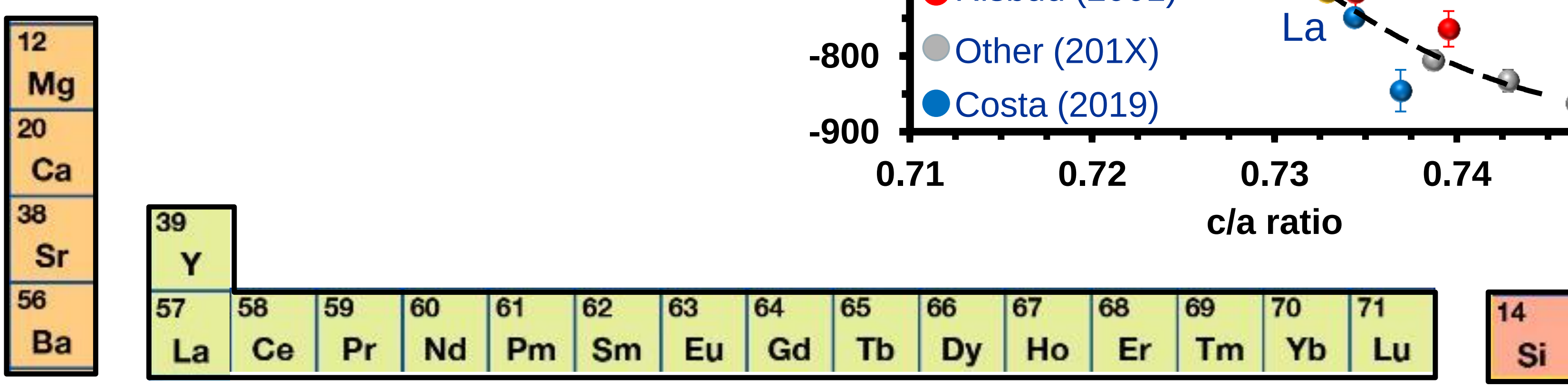

Stability of $AE_2RE_8(SiO_4)_6O_2$

- Apatite is a by-product of reaction with CMAS
  - More stable phase
- Costa (2019) → Enthalpy of formation (ΔH_f) of the apatites from the base oxides more stable with increasing c/a ratio
  - Either from an increasing AE or RE cation radius
  - Only indicates more stability than base oxides
- However, when incorporating water vapor reactions, bond energy plays a role
  - Shorter bonds → stronger bonds
- Influence of thermodynamics and kinetics on the stability of apatites in water vapor

AE = Alkaline element, RE = Rare Earth

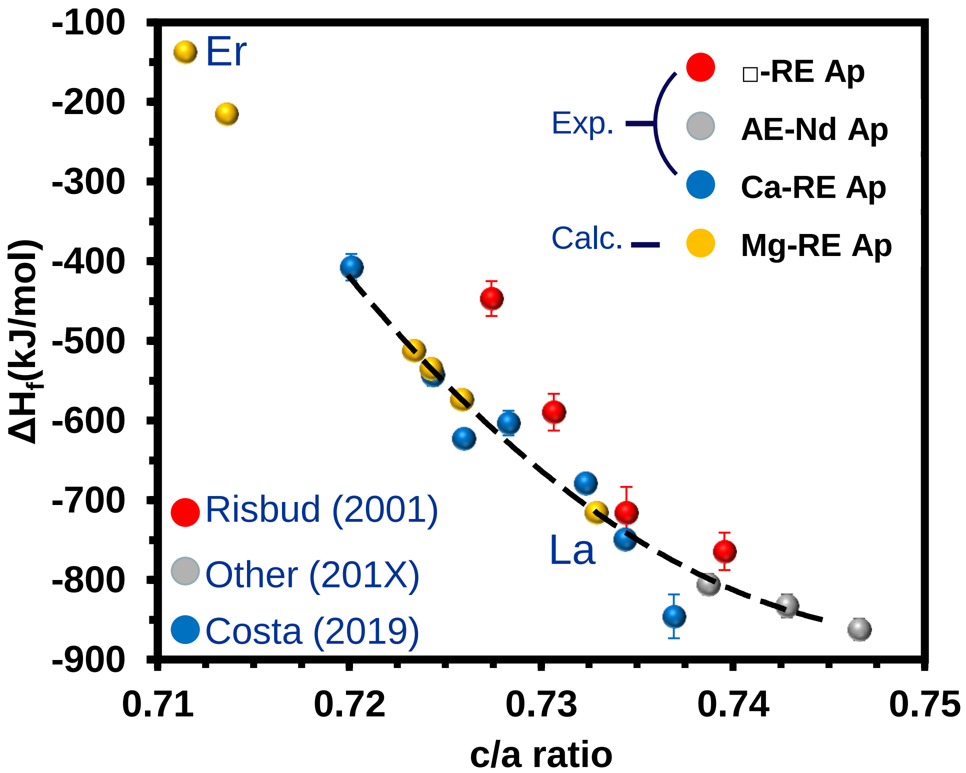

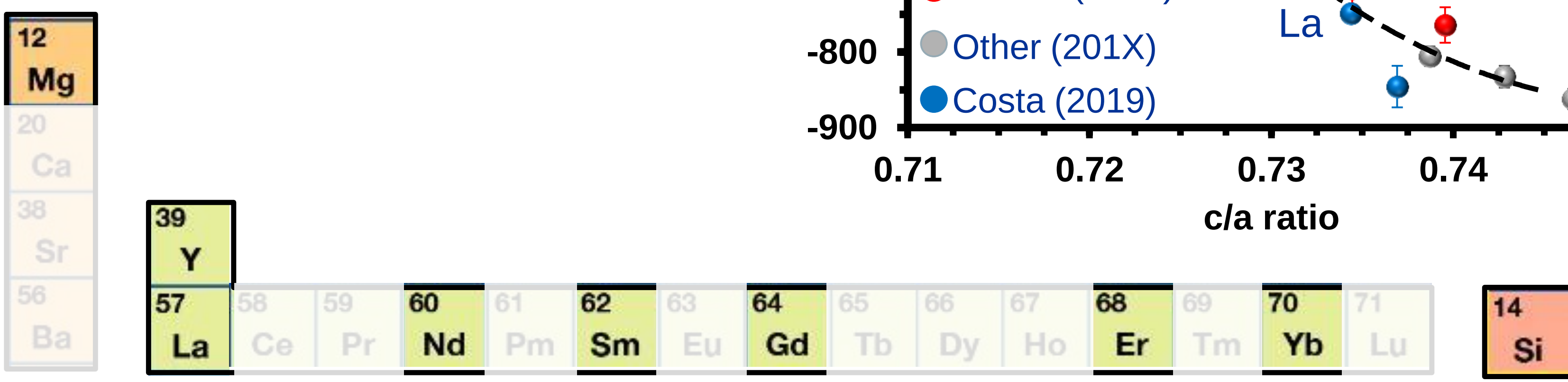

Processing, Measurements, and Characterization

- Solid state processing for pellets
  - 1700 °C sintering temperature in air for 6 hrs
- Characterize sample pre-exposure
  - Scanning electron microscopy (SEM)
  - Energy dispersive spectroscopy (EDS)
  - X-ray Diffraction (XRD)
  - CTE of samples with high temperature XRD

Steam Cycling conditions

- Test temperature: 1426°C
- 90%/10% H_2O/O_2
- 33 mm ID. Al_2O_3 tube
- 5 hr hot/20 min cold
- 15 total hot hours
- Velocity: ~10 cm/s

- Surface characterization post-exposure
  - XRD, SEM, EDS

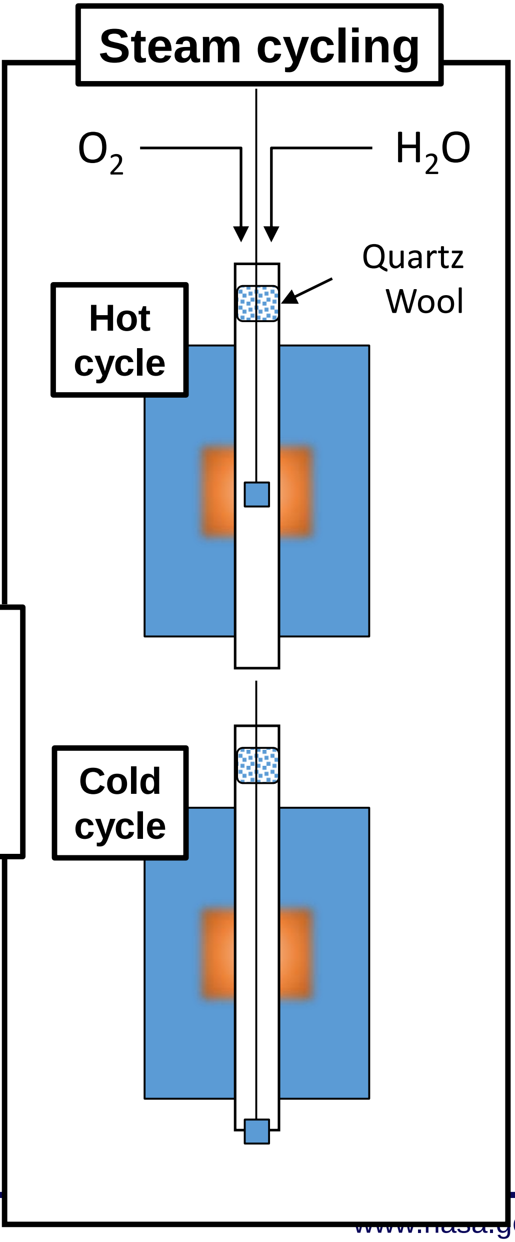

Scanning electron microscopy – Microstructure

- Of the RE = La, Nd, Sm, Gd, Er, Yb, Y processed only La, Nd, Sm, Gd, Y formed apatite, however
  - RE = La melted when sintered above 1580 °C
  - RE = Nd swelled prior to sintering due to humidity
  - RE = Er mainly formed Er_2SiO_5
  - RE = Yb formed a eutectic
- Apatite formed largely textured grain structure
- YbDS phase pure, but secondary phase at grain boundaries for Mg-RE apatites

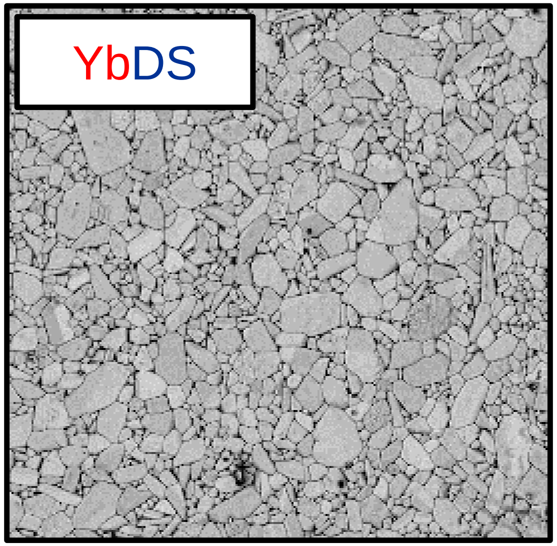

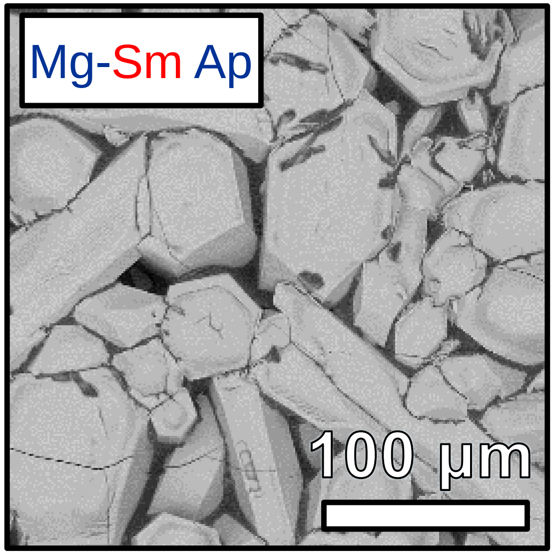

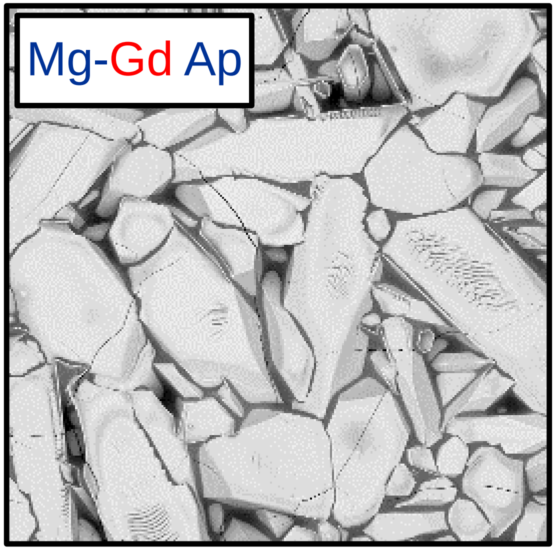

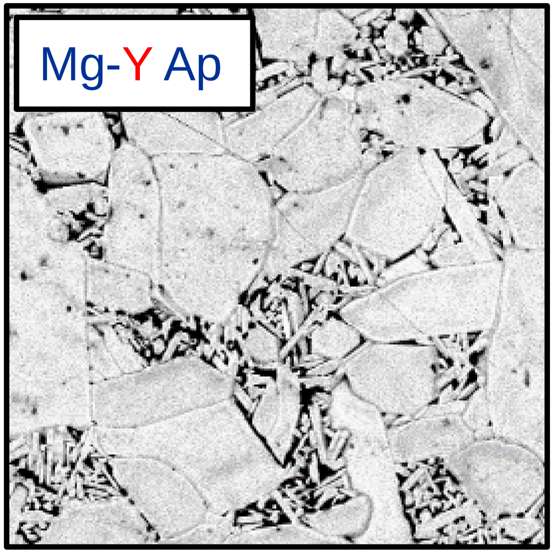

Energy Dispersive Spectroscopy – Secondary phases – as processed

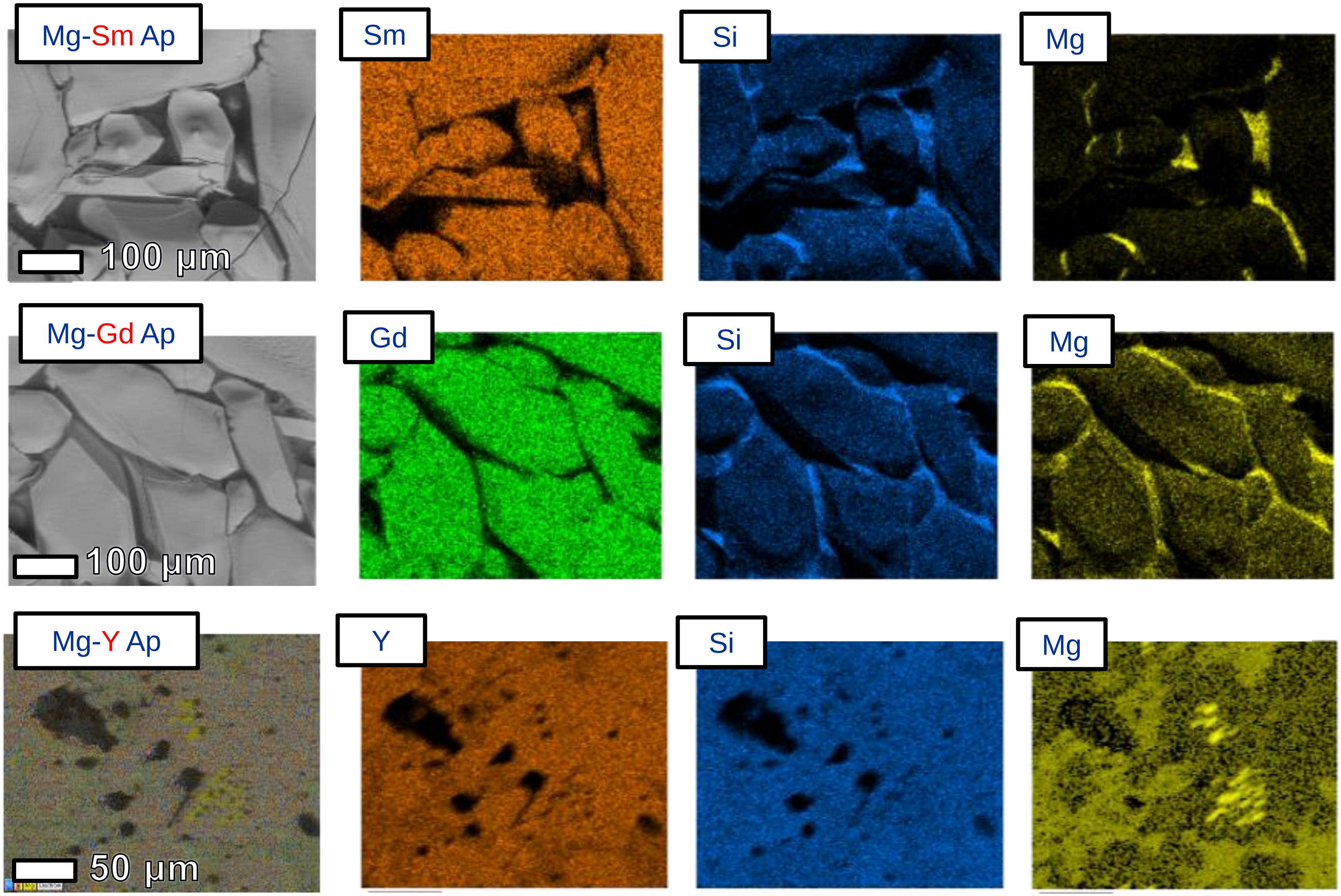

Energy Dispersive Spectroscopy – Secondary phases – as processed

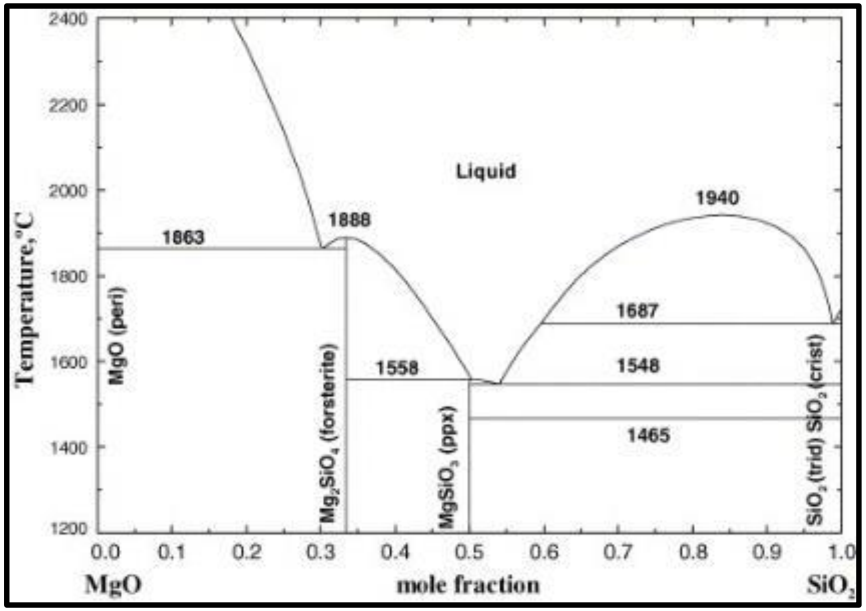

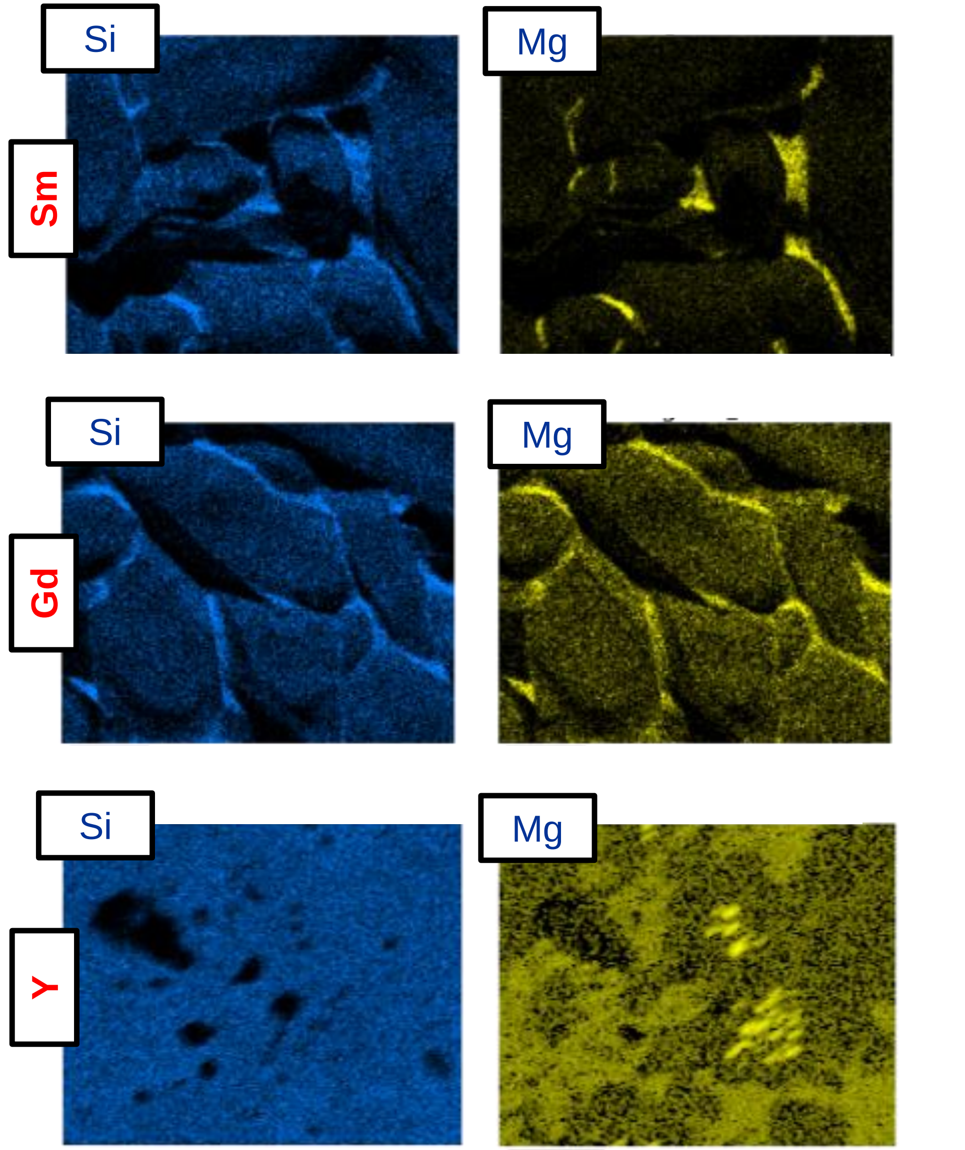

- RE = Sm forms forsterite (Mg_2SiO_4)
- RE = Gd forms enstatite ($MgSiO_3$)
- RE = Y forms precipitates of MgO and Y-monosilicate
- Secondary phases may also contribute to overall volatilization

X-ray Diffraction: Pre Steam Exposure

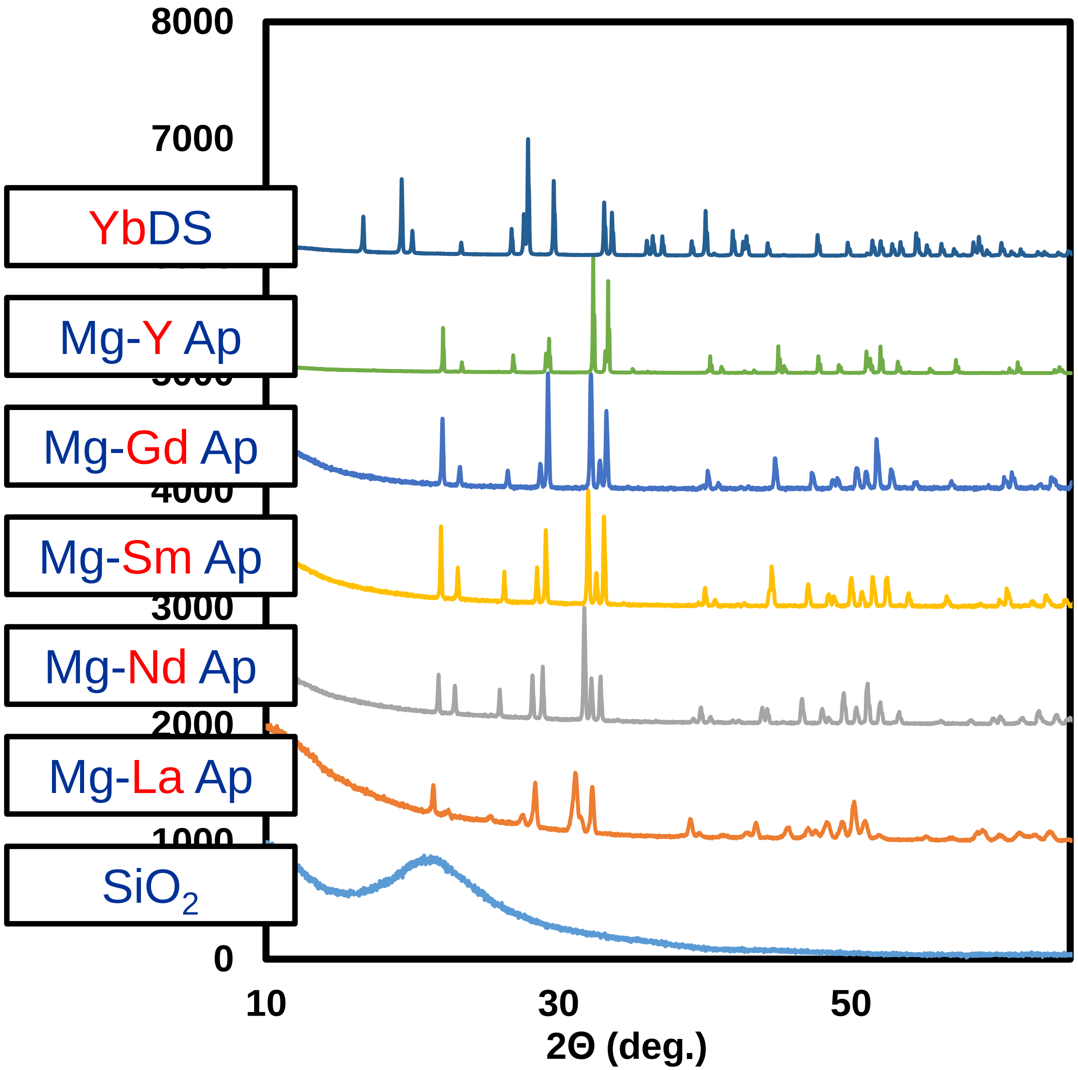

- XRD on sintered pellets
- SiO_2 → amorphous
- YbDS → phase pure
- Apatite formed for majority of REs, except for Er where Er_2SiO_5 formed instead
- Intergranular phase may be amorphous

High temperature XRD: Thermal expansion

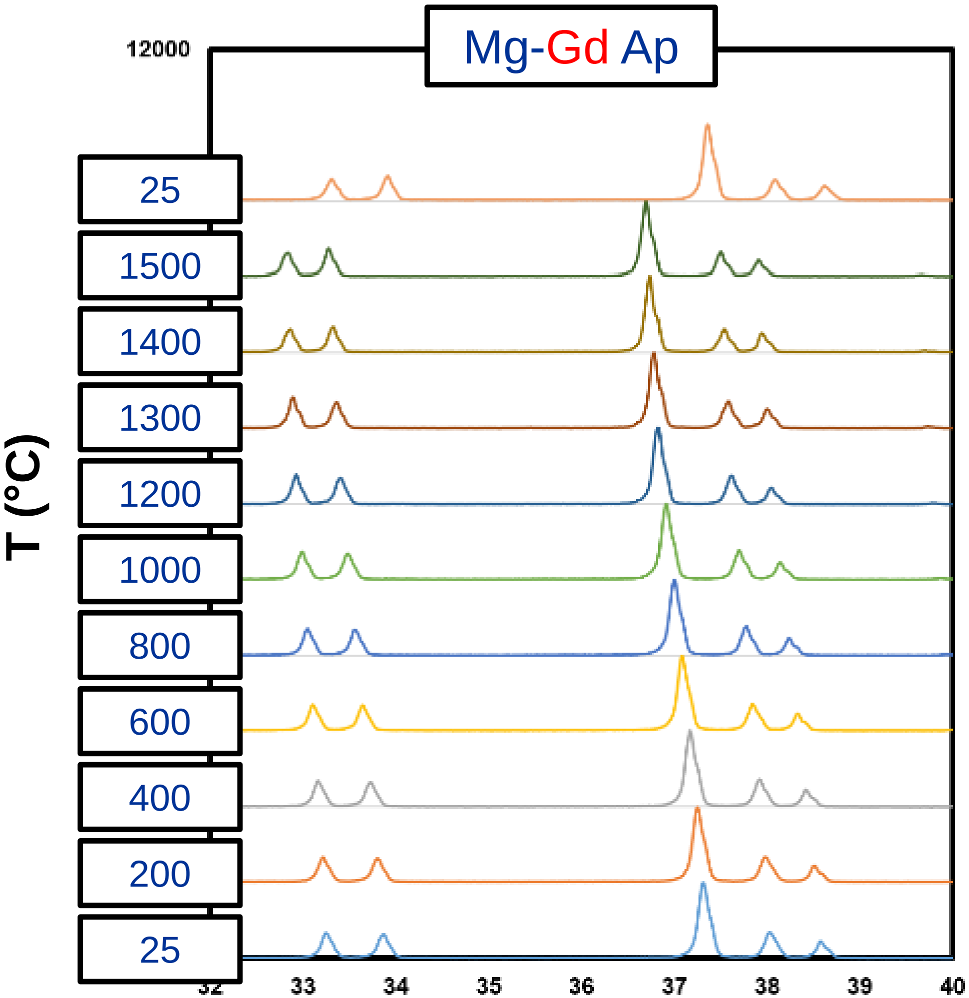

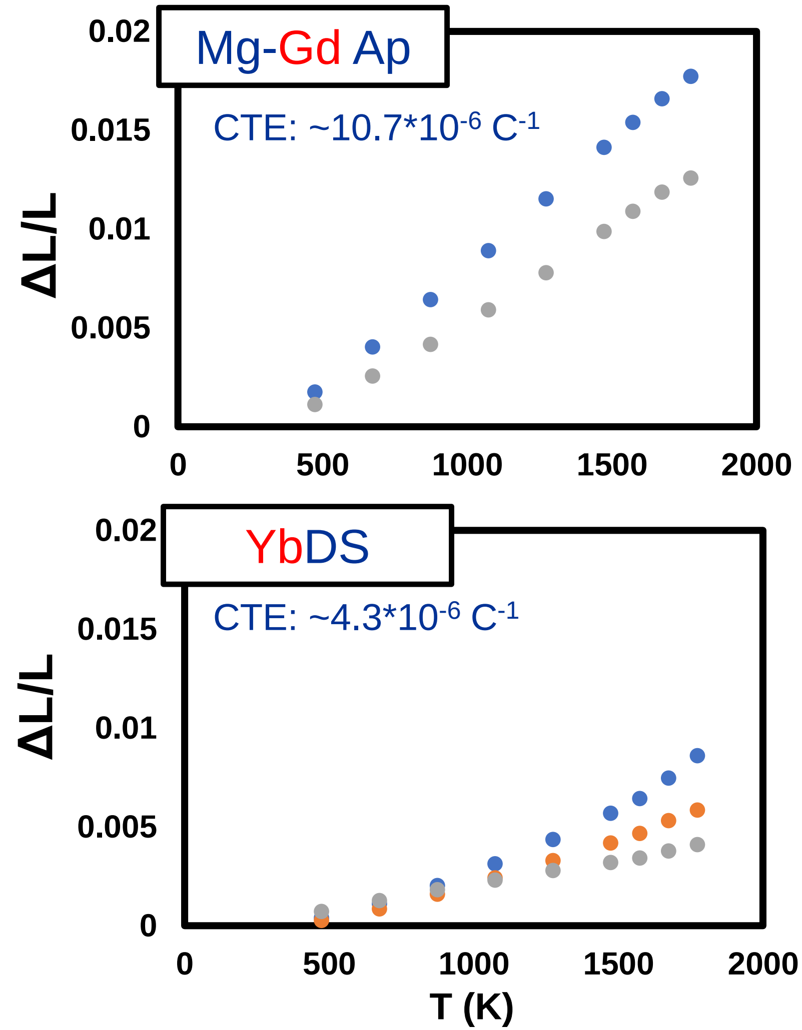

- Stable with temperature
- CTE too high, however...

High temperature XRD: Thermal expansion

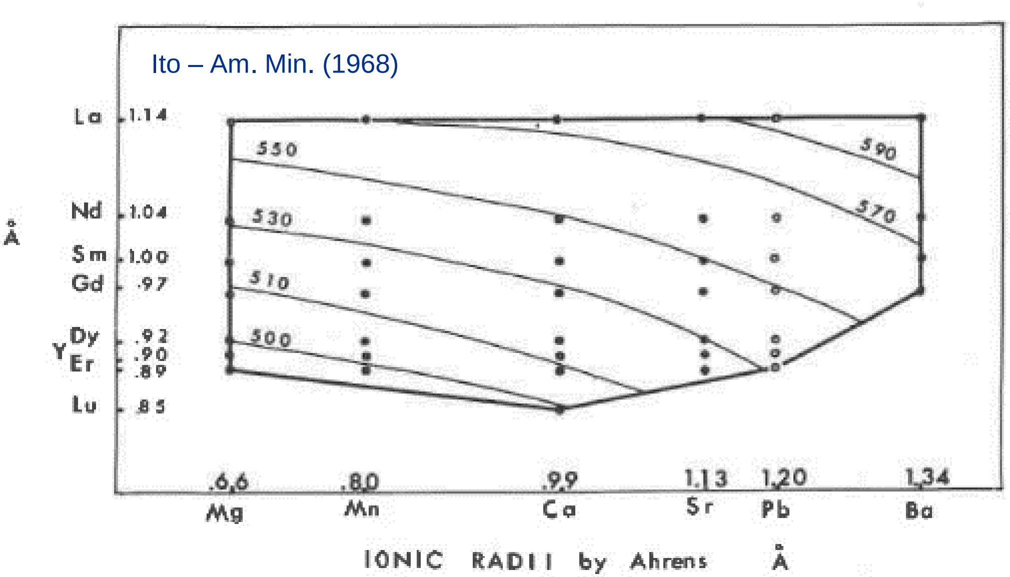

TABLE I. Linear expansion coefficients calculated at room temperature for $Ca_2La_8(SiO_4)_6O_2$ and $Ca_2Y_8(SiO_4)_6O_2$ crystals along the a' and c directions.

Crystal	Linear expansion coefficients	
	a'	c
$Ca_2La_8(SiO_4)_6O_2$	8.9×10^{-6} K^{-1}	6.6×10^{-6} K^{-1}
$Ca_2Y_8(SiO_4)_6O_2$	7.1×10^{-6} K^{-1}	5.1×10^{-6} K^{-1}

Hopkins J. Appl Phys (1973)

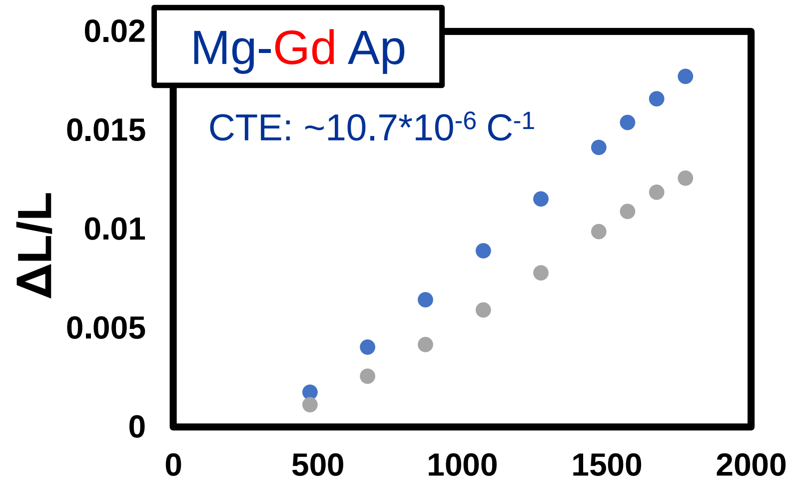

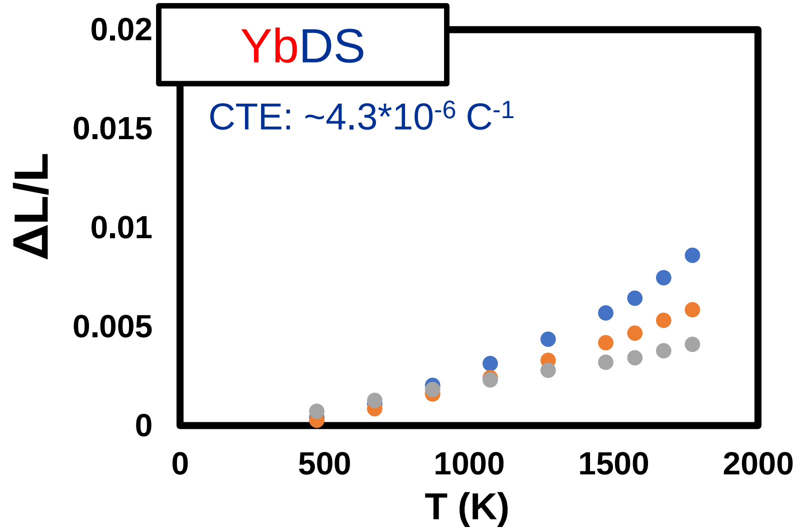

- Ptacek – Ceramics Int'l (2015) – $Sr_2Y_8(SiO_4)_6O_2$ – $1.1*10^{-6}$ C^{-1}

Recession in water vapor

- 5hr hot cycle, 3 cycles → 15 total hrs
  - Secondary phase at grain boundary may contribute to volatilization

Sample	Recession rate $(mg/cm^2 \cdot hr)*10^3$
YbDS	-8.7
Mg-Y Ap	-8.4
Mg-Gd Ap	-38.0
Mg-Sm Ap	-25.0
SiO_2	-49.0

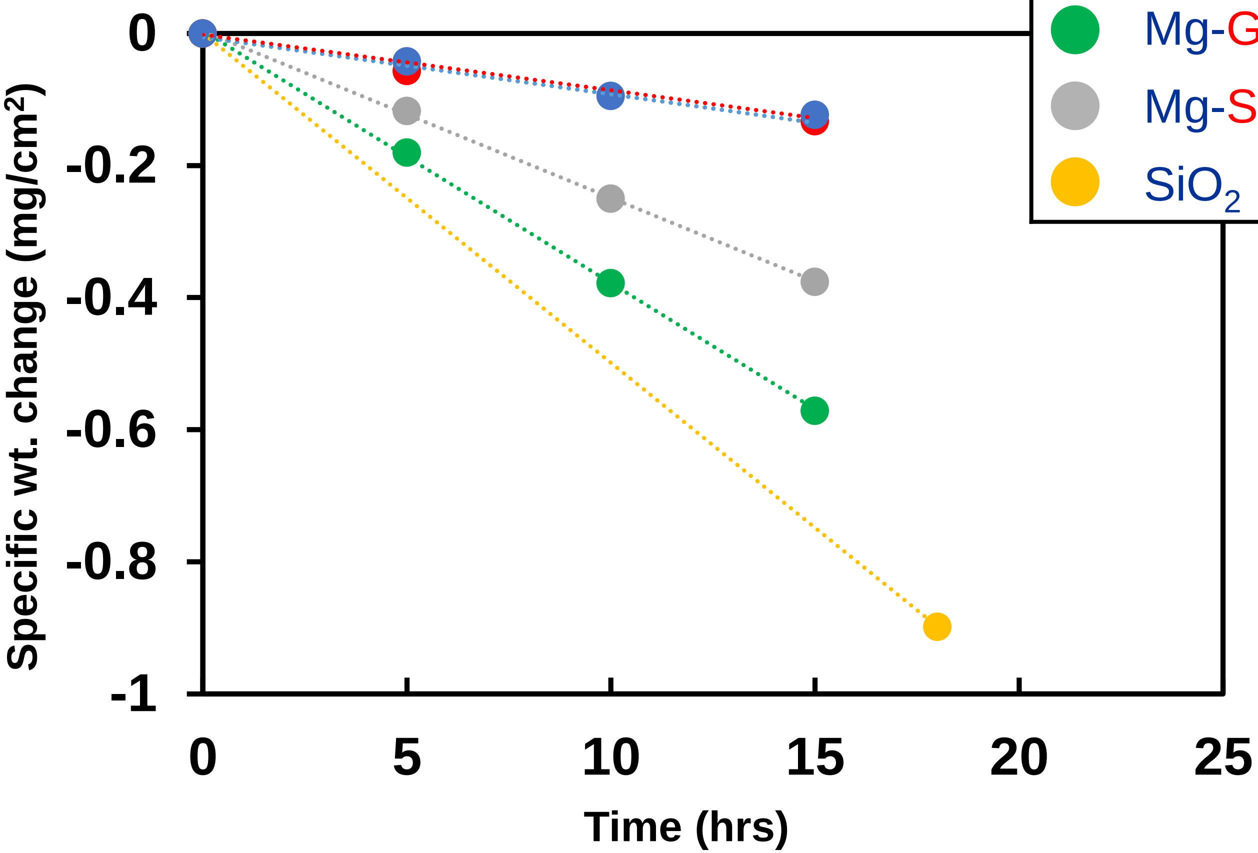

Recession in water vapor

- 5hr hot cycle, 3 cycles → 15 total hrs
  - Secondary phase at grain boundary may contribute to volatilization

Sample	Recession rate $(mg/cm^2 \cdot hr)*10^3$
YbDS	-8.7
Mg-Y Ap	-8.4
Mg-Gd Ap	-38.0
Mg-Sm Ap	-25.0
SiO_2	-49.0

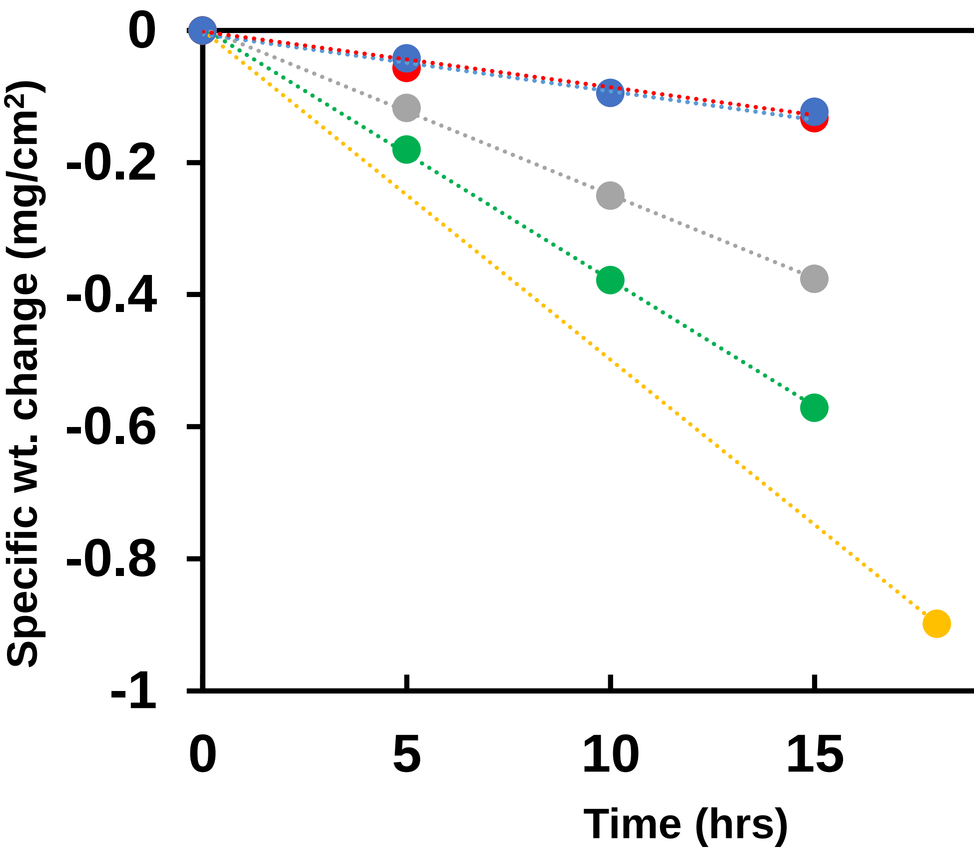

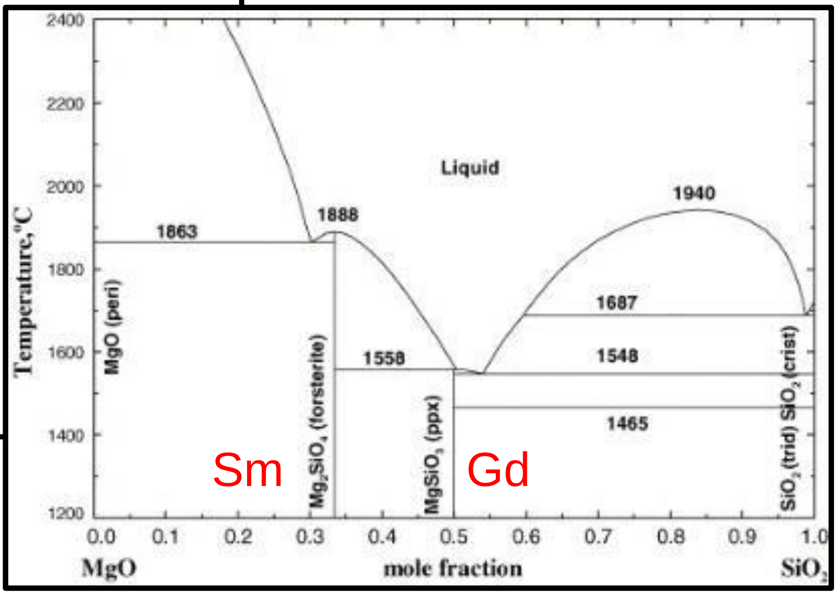

Recession in water vapor

- 5hr hot cycle, 3 cycles → 15 total hrs
  - Secondary phase at grain boundary may contribute to volatilization

Sample	Recession rate $(mg/cm^2 \cdot hr)*10^3$
YbDS	-8.7
Mg-Y Ap	-8.4
Mg-Gd Ap	-38.0
Mg-Sm Ap	-25.0
SiO_2	-49.0

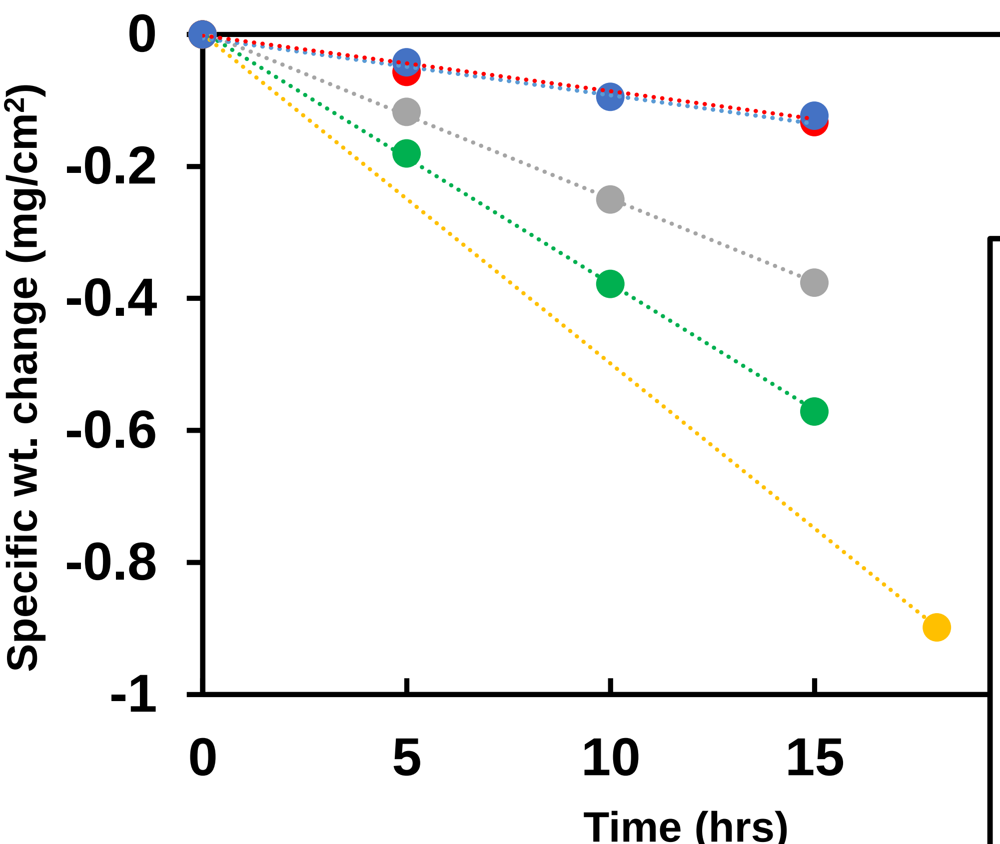

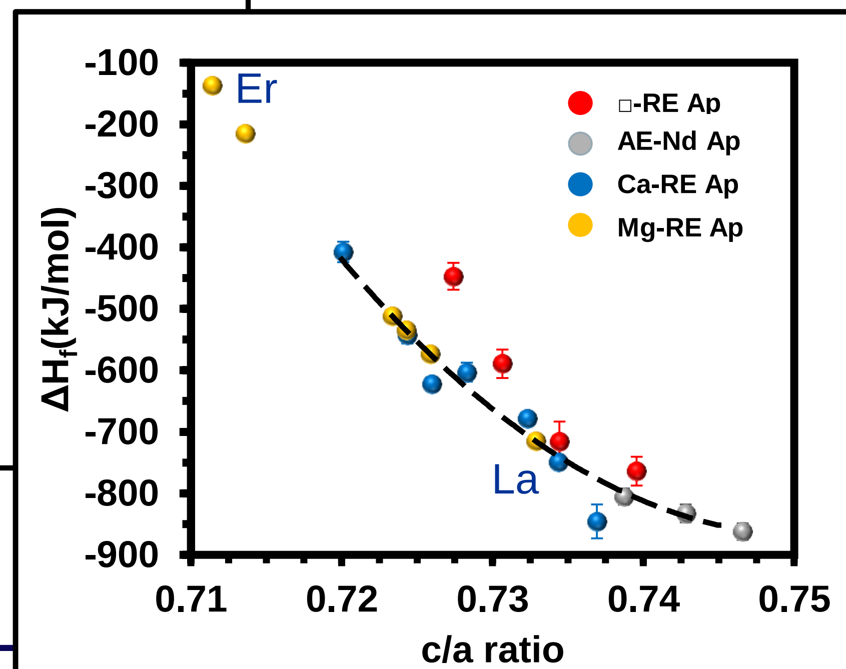

Mg-Gd apatite pre and post-exposure

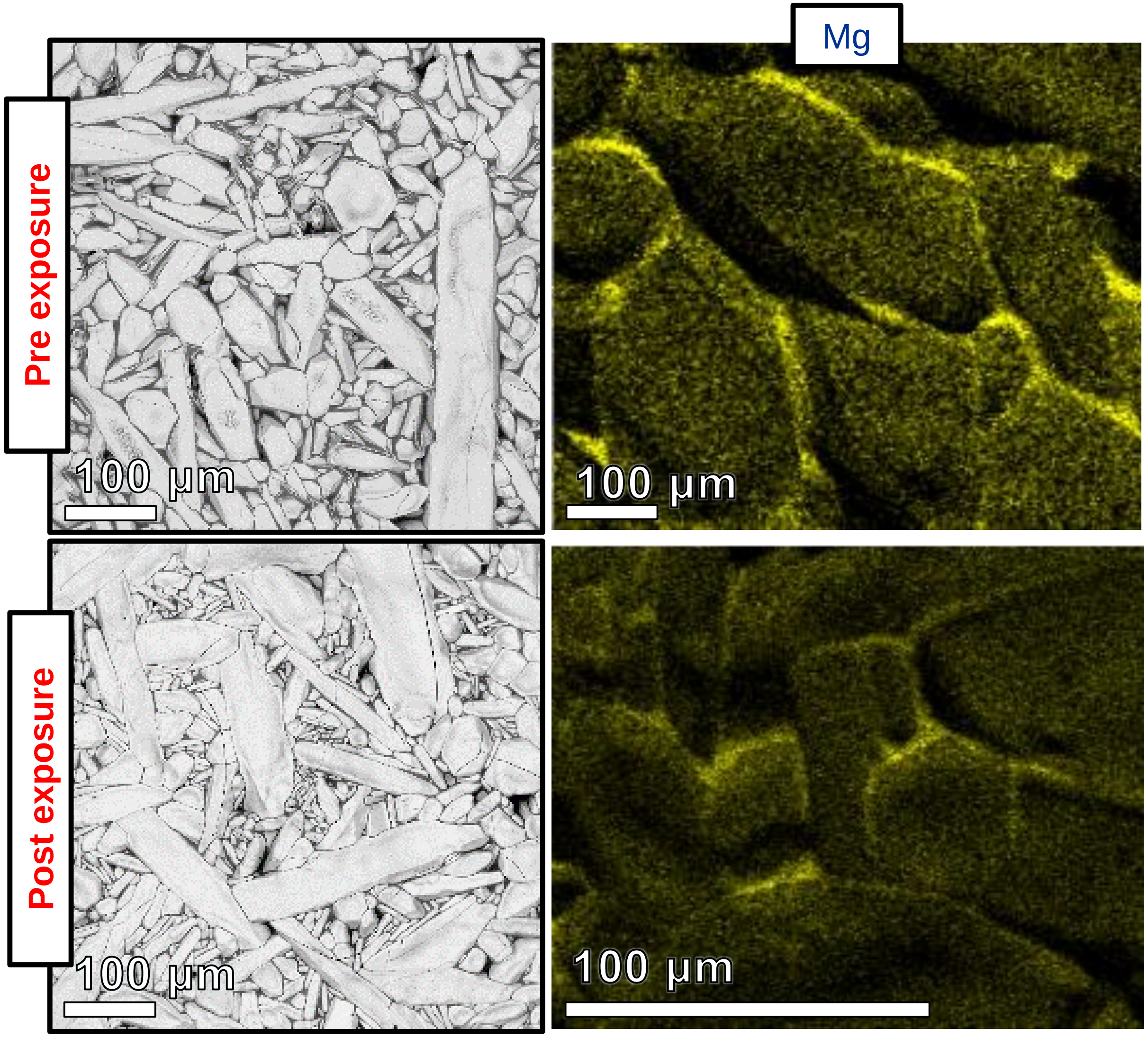

- Bimodal separation of grain size increased after exposure
- Grain boundary phase reduces in size after exposure
  - 10 µm → 2 µm thickness
- Minor change in composition of apatite measured by EDS

XRD comparison after HT steam exposure

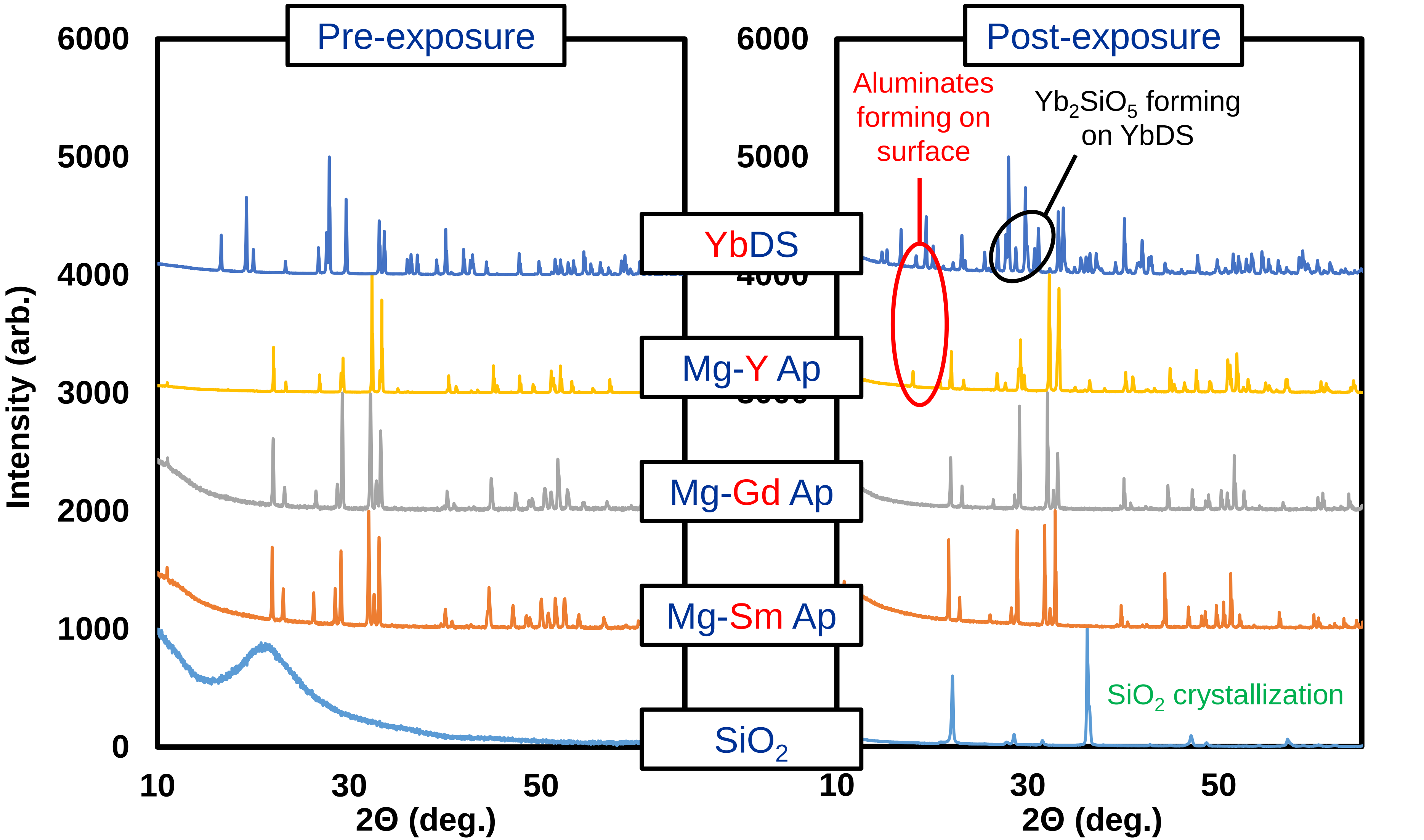

XRD comparison after HT steam exposure

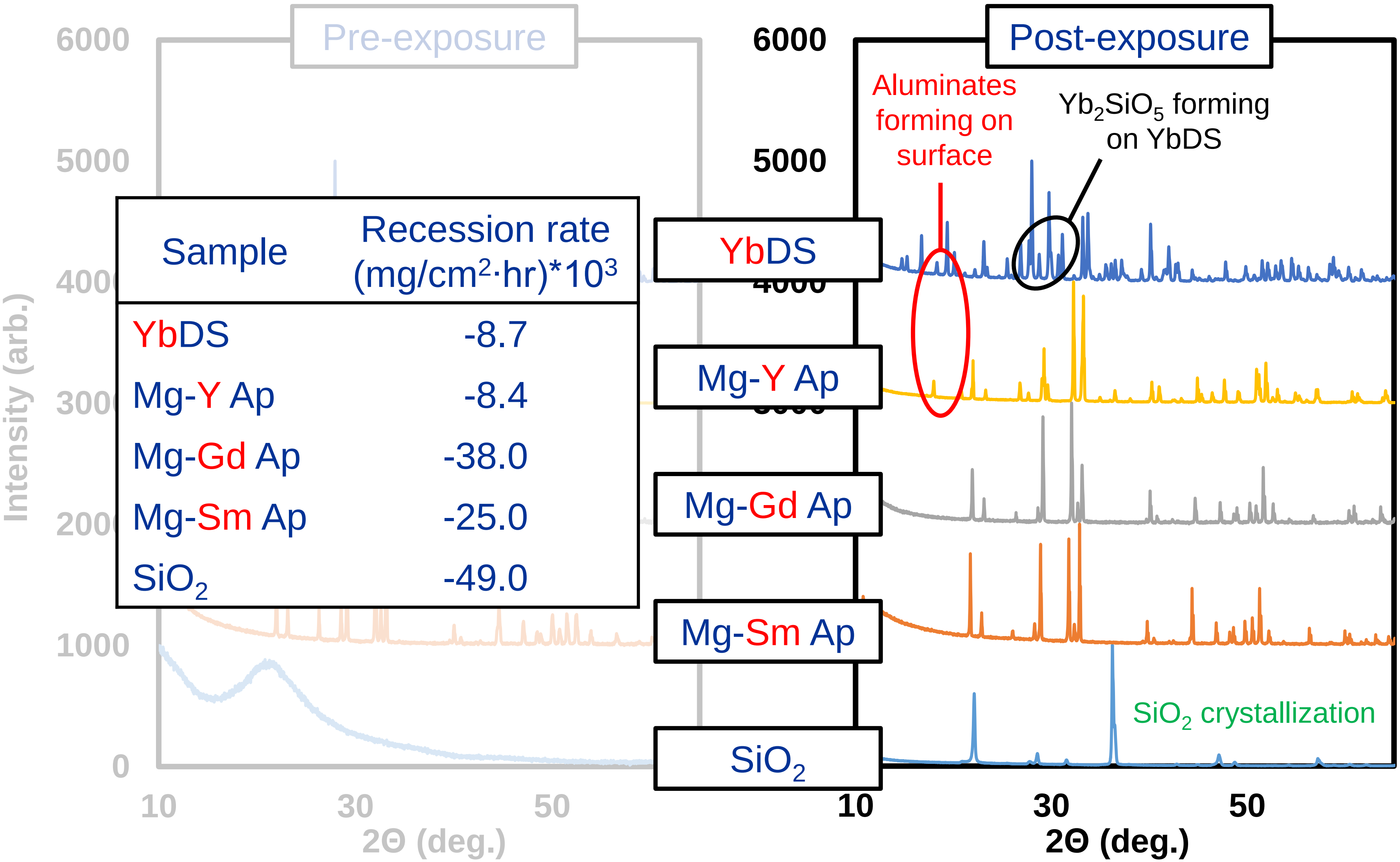

Sample	Recession rate (mg/cm²·hr)*10³
YbDS	-8.7
Mg-Y Ap	-8.4
Mg-Gd Ap	-38.0
Mg-Sm Ap	-25.0
SiO_2	-49.0

XRD comparison after HT steam exposure

- Shift in XRD peak positions indicates possible strain/compositional effects

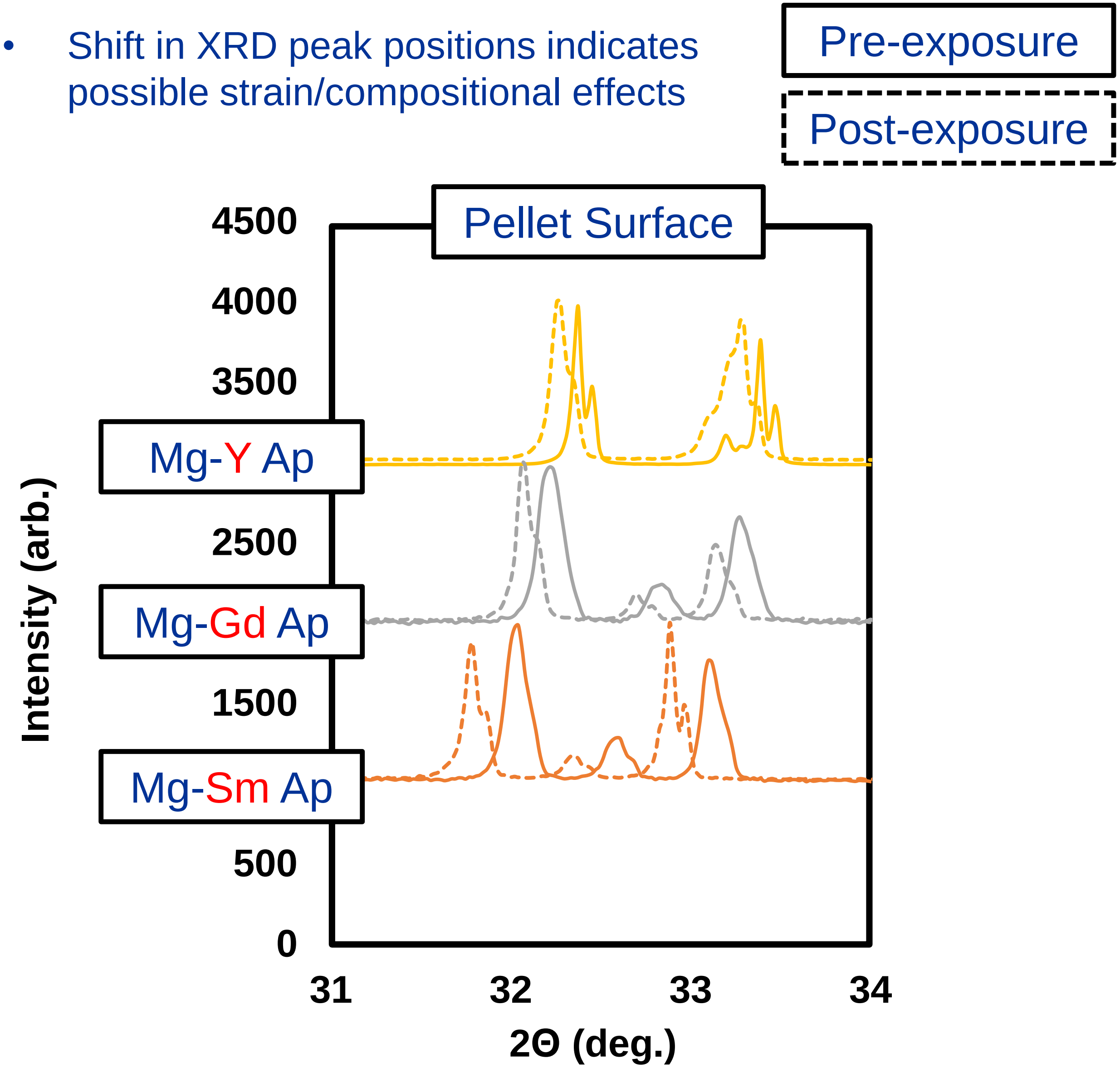

XRD comparison after HT steam exposure

- Shift in XRD peak positions indicates possible strain/compositional effects due to secondary phases
- Apatite remains thermodynamically stable phase

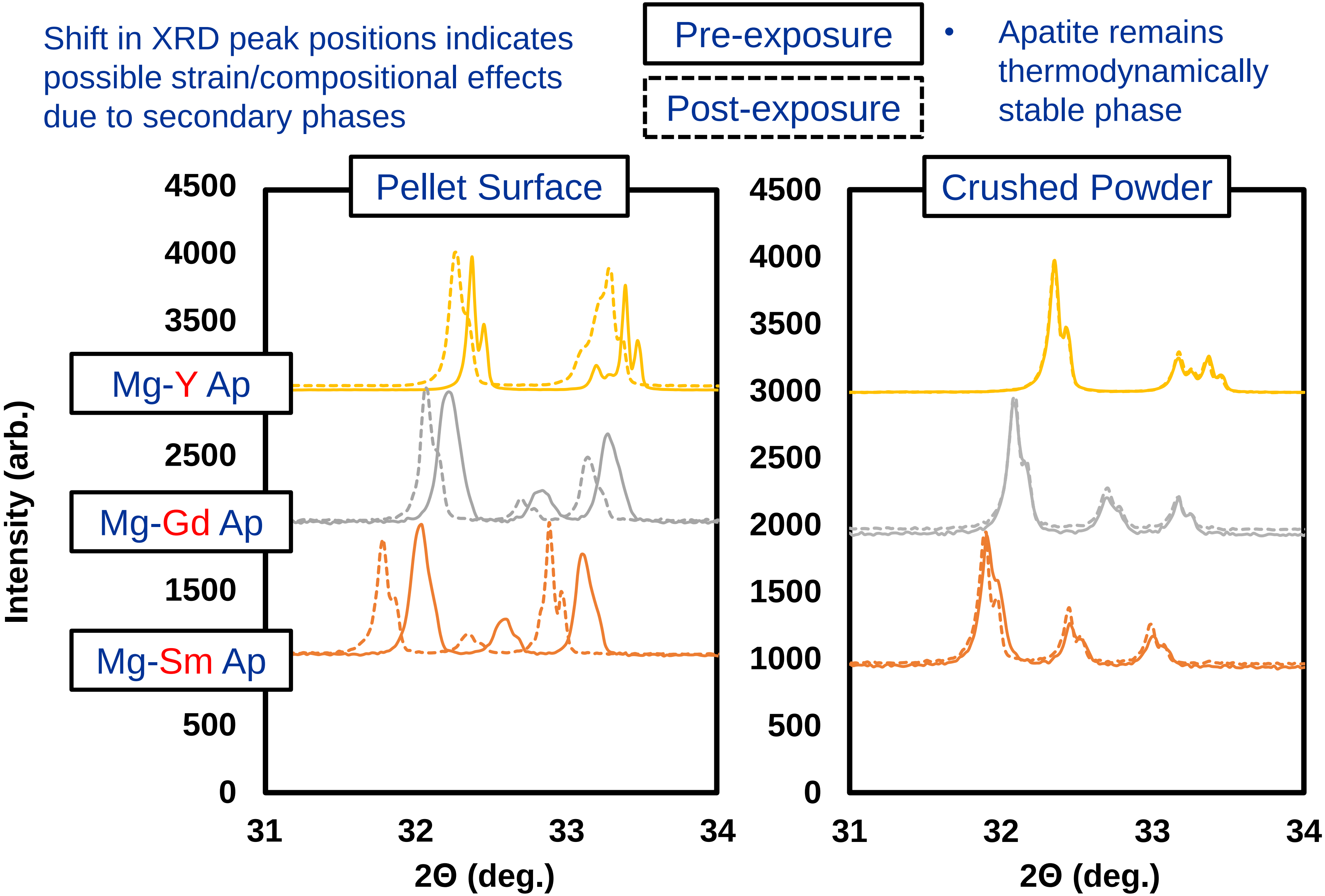

Conclusions

- Mg moves window of stabilization towards larger cations
  - La, Sm, Nd, etc.
- Apatite phase forms, but a secondary MgO-containing phase at grain boundaries
- Thermodynamic stability doesn’t fully describe the kinetic behavior when exposed to water vapor
- MgY apatite has similar recession to that of YbDS
- *Future work*
  - Investigate/control intergranular phase
  - Tune CTE with doping
  - Pursue CMAS studies

Thank you for listening

Special thanks to:

Bryan Harder

Gustavo Costa

Rick Rogers

ICACC 2020
Daytona Beach, FL
01 / 26-31 / 2020

ICACC 2020

Daytona Beach, FL

01 / 26-31 / 2020

Future Work – CMAS exposure

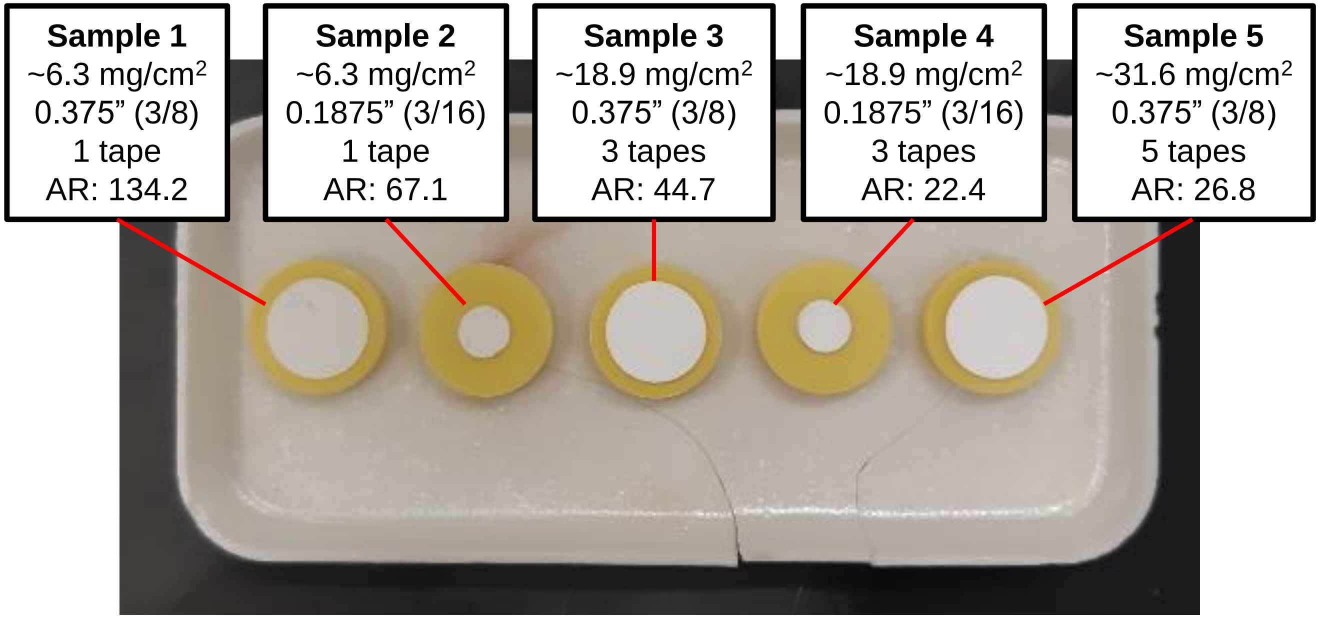

Future Work – CMAS exposure

Sample 1	Sample 2	Sample 3	Sample 4	Sample 5
~6.3 mg/cm^2	~6.3 mg/cm^2	~18.9 mg/cm^2	~18.9 mg/cm^2	~31.6 mg/cm^2
0.375” (3/8)	0.1875” (3/16)	0.375” (3/8)	0.1875” (3/16)	0.375” (3/8)
1 tape	1 tape	3 tapes	3 tapes	5 tapes
AR: 134.2	AR: 67.1	AR: 44.7	AR: 22.4	AR: 26.8